

# Electrostatic Forces and Dielectric Polarizability of Multiply Protonated Gas-Phase Cytochrome *c* Ions Probed by Ion/Molecule Chemistry

Paul D. Schnier, Deborah S. Gross, and Evan R. Williams\*

Contribution from the Department of Chemistry, University of California, Berkeley, California 94720

Received September 23, 1994<sup>Ⓢ</sup>

**Abstract:** We demonstrate a method to quantitatively determine both Coulomb energy and the intrinsic dielectric polarizability of large, multiply protonated gas-phase protein ions. Information about the conformation and maximum charge state of these ions in the gas phase is also obtained. The apparent gas-phase basicities (GB<sup>app</sup>) of individual charge states are measured; these values are compared to those calculated from a relatively simple model in which charges are assigned to sites in an ion such that the overall ion free energy is minimized. For cytochrome *c*, we find our calculations can be fit to measured values of GB<sup>app</sup> of the 3+ to 15+ ions using a fully denatured ion conformation and an  $\epsilon_r = 2.0 \pm 0.2$ . This value is substantially higher than that of the small cyclic decapeptide gramicidin *s*, but below that predicted by theory for the interior of a protein. We find that the intrinsic basicity of individual basic charge sites, estimated by GB measurements of small peptides, is 13–18 kcal/mol higher than those of the corresponding individual amino acid, consistent with independent intramolecular interaction (self-solvation) of the charge site occurring in these large multiply protonated ions. For the 21+ ion in a denatured conformation, we find that the minimum Coulomb contribution to ion zero-point energy is 24 eV. This substantial Coulomb energy accounts for the increased reactivity and decreased stability of these highly charged ions. Our calculations indicate that the maximum charge state observed in electrospray mass spectra is determined by the relative apparent gas-phase basicity of the ion/solvent combination. Finally, we find that the gas-phase conformation of cytochrome *c* ions is consistent with a denatured form, although our calculations indicate that cytochrome *c* electrospayed from an aqueous solution is initially in its native conformation subsequent to its desorption into the gas phase.

## Introduction

Electrostatic forces are long-range interactions that play a key role in the conformation and function of biomolecules. These forces are reduced or shielded by the dielectric polarizability of the media between the charges. Accurate values of the effective shielding between charges in a biomolecule are important for understanding processes in which intramolecular electrostatic forces play a role, including intramolecular electron transfer,<sup>1</sup> protein folding,<sup>2</sup> and the reactivity and dissociation<sup>3–5</sup> of gas-phase multiply protonated ions. In combination with tandem mass spectrometry, the latter has shown tremendous promise for the direct sequencing of large (>10<sup>4</sup> Da) DNA<sup>4</sup> and protein molecules.<sup>5</sup>

Determining the magnitude of the effective dielectric polarizability ( $\epsilon_{\text{eff}}$ ) between charges in biomolecules presents a difficult challenge for both experiment<sup>6,7</sup> and theory.<sup>8–11</sup> Values for the bulk dielectric constant of a protein, measured by

applying a weak electric field to bulk protein powder, range from 1.6 to 3.5 for various proteins.<sup>6</sup> These average values are of limited use in describing interactions of specific charges in the interior of a protein.<sup>8</sup> Water, which has a bulk dielectric constant of 78, has a significant effect on  $\epsilon_{\text{eff}}$ , even for charge interactions in the interior of the protein. Electrochemical measurements on native cytochrome *c* in aqueous solution indicate  $\epsilon_{\text{eff}} = 40–60$  for electrostatic interactions between modified exterior lysines and the interior heme iron.<sup>7</sup>

A number of theoretical approaches for calculating  $\epsilon_{\text{eff}}$  have been developed.<sup>8–11</sup> One commonly used method is the macroscopic continuum dielectric model,<sup>10</sup> in which the protein is represented by a region of low dielectric constant surrounded by a high dielectric medium. Values of 2–4 for native proteins have been calculated<sup>11</sup> and are used for the low dielectric constant representing the protein interior in this model. Electrochemical reduction potentials of modified and wild-type

\* Author to whom correspondence should be addressed.

<sup>Ⓢ</sup> Abstract published in *Advance ACS Abstracts*, June 1, 1995.

(1) (a) Bolton, J. R.; Mataga, N.; McLendon, G. L., Eds. *Electron Transfer in Inorganic, Organic, and Biological Systems*; Adv. Chem. Ser. 228; American Chemical Society: Washington, DC, 1991. (b) Steffen, M. A.; Boxer, S. G. *Science* **1994**, *264*, 810–816.

(2) Creighton, T. E. *Proteins*, 2nd ed.; W. H. Freeman & Co.: New York, 1993.

(3) (a) Loo, J. A.; Edmonds, C. G.; Udseth, H. R.; Smith, R. D. *Anal. Chim. Acta* **1990**, *241*, 167–173. (b) Rockwood, A. L.; Busman, M.; Smith, R. D. *Int. J. Mass Spectrom. Ion Processes* **1991**, *111*, 103–129. (c) Smith, R. D.; Barinaga, C. J.; Udseth, H. R. *J. Phys. Chem.* **1989**, *93*, 5019–5022.

(4) (a) McLuckey, S. A.; Habibigoudarzi, S. *J. Am. Chem. Soc.* **1993**, *115*, 12085–12095. (b) McLuckey, S. A.; Van Berkel, G. J.; Glush, G. L. *J. Am. Soc. Mass Spectrom.* **1992**, *3*, 60–70.

(5) Senko, M. W.; Beu, S. C.; McLafferty, F. W. *Anal. Chem.* **1994**, *66*, 415–417.

(6) (a) Rosen, D. *Trans. Faraday Soc.* **1963**, *59*, 2178–2191. (b) Takashima, S.; Schwan, H. P. *J. Phys. Chem.* **1965**, *69*, 4176–4182. (c) Harvey, S. C.; Hoekstra, P. J. *Phys. Chem.* **1972**, *76*, 2987–2994. (d) Bone, S.; Pethig, R. *J. Mol. Biol.* **1982**, *157*, 571–575.

(7) Rees, D. C. *J. Mol. Biol.* **1980**, *141*, 323–326.

(8) (a) King, G.; Lee, F. S.; Warshel, A. *J. Chem. Phys.* **1991**, *95*, 4366–4377. (b) Warshel, A.; Åqvist, J. *Annu. Rev. Biophys. Chem.* **1991**, *20*, 267–298. (c) Warshel, A.; Russel, S. T.; Churg, A. K. *Proc. Natl. Acad. Sci. U.S.A.* **1984**, *81*, 4785–4789.

(9) Krishtalik, L. I. *J. Theor. Biol.* **1989**, *139*, 143–154.

(10) (a) Tanford, C.; Kirkwood, J. G. *J. Am. Chem. Soc.* **1957**, *79*, 5333–5339. (b) Sharp, K. A.; Honig, B. *Annu. Rev. Biophys. Chem.* **1991**, *19*, 301–332. (c) Gilson, M. K.; Rashin, A.; Fine, R.; Honig, B. *J. Mol. Biol.* **1985**, *183*, 503–516. (d) Jayaram, B.; Sharp, K. A.; Honig, B. *Biopolymers* **1988**, *28*, 975–993.

(11) (a) Gilson, M. K.; Honig, B. *Biopolymers* **1986**, *25*, 2097–2119. (b) Pethig, R. *Dielectric and Electronic Properties of Biological Materials*; John Wiley and Sons: New York, 1979.

cytochrome *b*<sub>5</sub> are consistent with this model using a dielectric constant of 2–4 for the protein interior.<sup>12</sup> The dielectric constant of bulk water is typically used for the surrounding medium for a protein in aqueous solution. Microscopic simulations by Warshel and co-workers<sup>8</sup> include the effects of the surrounding water which is treated as a reaction field. The effect of the reaction field is to increase the dielectric polarizability of the interior of the protein itself; values as large as 10 have been calculated for regions of catalytic importance.<sup>8a</sup>

Multiply protonated gas-phase ions, such as those produced by electrospray ionization, are ideally suited for the investigation of the intrinsic electrostatic properties of charged biomolecules in the absence of water. Effects of multiple charge on ion reactivity and dissociation have been studied for many years.<sup>13</sup> More recently, effects of multiple protonation on rates of proton transfer<sup>14,15</sup> and deuterium exchange,<sup>16</sup> collisional cross sections,<sup>17</sup> and dissociation<sup>4,5</sup> of biomolecules have been reported. Increased rates of proton transfer with increasing charge state have been observed and attributed to increasing Coulomb repulsion as well as decreasing intrinsic basicity of sites of protonation.<sup>14</sup> For example, McLuckey, Van Berkel, and Glish<sup>14a</sup> found the proton transfer rates for 9+ to 15+ ions of cytochrome *c* to neutral dimethylamine increased from  $<2 \times 10^{-12}$  to  $9 \times 10^{-10}$  cm<sup>3</sup>/(mol·s). Similar results have been reported by Cassady *et al.*<sup>14c</sup> for proton transfer from isolated ubiquitin ions to four reference bases. The gas-phase conformation of various charge states of protein ions has been probed using gas-phase deuterium exchange,<sup>16</sup> collisional cross section,<sup>17</sup> and proton transfer reactions.<sup>15</sup>

In addition to increased rates of proton transfer, higher charge states of ions are more readily dissociated.<sup>3c</sup> The effects of multiple charges on lowering bond dissociation energies have been modeled by Rockwood *et al.*<sup>3b</sup> using a linear “charge on a string” model in which charges are evenly distributed and the dielectric polarizability is one.

We have proposed a method<sup>18,19</sup> to quantitatively measure both Coulomb energy and the intrinsic dielectric polarizability ( $\epsilon_r$ ) of gas-phase multiply protonated ions. This method was recently demonstrated for the doubly protonated ion of gramicidin *s* for which values of Coulomb energy  $>27.9$  kcal/mol and  $\epsilon_r <1.2$  were obtained.<sup>18</sup> For doubly protonated 1,*n*-diaminoalkanes ( $n = 7-10, 12$ ), Coulomb energy was found to decrease from 29.4 to 19.8 kcal/mol for  $n = 7$  to 12, and an

average  $\epsilon_r = 1.01 \pm 0.07$  was obtained.<sup>19</sup> The low value of  $\epsilon_r$  indicates that shielding between charges in these relatively small gas-phase ions is negligible, presumably due to effects of the surrounding medium which is vacuum (vacuum permittivity = 1.00).

Here, we present results for the multiply protonated protein cytochrome *c*. Experimental measurements of the apparent gas-phase basicity (GP<sup>app</sup>) of the individual charge states 3+ to 15+ of cytochrome *c* are reported. These values are fit to a relatively simple model used to calculate the lowest free energy configuration of charges for each charge state. This makes possible the determination of a lower limit of the dielectric polarizability of gas-phase cytochrome *c* ions and provides information about their conformation. These are the first experimental measurements of Coulomb energy in a multiply protonated protein ion; by comparison to calculations using the relatively simple model presented here, information about the intrinsic dielectric polarizability of a protein in the complete absence of water, *i.e.* vacuum, is obtained.

## Experimental Section

**Instrumentation.** Experimental measurements of gas-phase basicity are performed on a 2.74 T external ion source ESI-FTMS described elsewhere.<sup>18</sup> Ions are desolvated in the electrospray source using a stainless-steel capillary heated to 200 °C.<sup>20</sup> A series of electrostatic lenses (–2.2 kV maximum) guide ions from the source to the FTMS ion cell in which a base pressure of  $7 \times 10^{-9}$  Torr is maintained. Ions are collisionally trapped in the cell using N<sub>2</sub> gas introduced through a pulsed valve to a pressure of approximately  $2 \times 10^{-6}$  Torr. A potential of 6.0 V is applied to the trapping plates during ion accumulation<sup>21</sup> and is subsequently reduced to 1.0 V during ion excitation and detection. Ions are detected using an rf excitation sweep (120 V peak-to-peak, 1100 Hz/μs, low to high frequency) and 128K data points are acquired.

Equine cytochrome *c* (Sigma Chemical Co., St. Louis, MO) is electrosprayed both from a 49.5%/49.5%/1% water/methanol/acetic acid solution and from 100% water at a concentration of  $4 \times 10^{-5}$  M. All peptides, with the exception of Hu-ras<sup>Ha</sup> (sequence GAGGVGKS, Peninsula Laboratories, Belmont, CA), were obtained from Sigma Chemical Co. The peptides are electrosprayed from methanol at concentrations of  $\sim 1 \times 10^{-5}$  M. A flow rate of 2.0 μL/min is used for all solutions. All neutral reference bases<sup>22</sup> were obtained from Aldrich Chemical Co. (Milwaukee, WI) and are introduced into the mass spectrometer through a sapphire leak valve (Varian Vacuum Products, Lexington, MA) after several freeze–pump–thaw cycles for degassing.

**Measured Apparent Gas-Phase Basicity.** The bracketing method<sup>23</sup> is used to determine the apparent gas-phase basicity (GB<sup>app</sup>) of each charge state of cytochrome *c*. With this method, an ion of unknown basicity is isolated and reacted with a neutral base of known GB. Proton transfer from the ion to the neutral base indicates the relative GB<sup>app</sup> of the two species. Molecular ions of cytochrome *c* are accumulated in the FTMS cell for 10 s. Individual charge states are isolated using SWIFT<sup>24</sup> and reacted with the reference bases listed in Table 1 for

(12) Rodgers, K. K.; Sligar, S. G. *J. Am. Chem. Soc.* **1991**, *113*, 9419–9421.

(13) (a) Ast, T.; Beynon, J. H.; Cooks, R. G. *Org. Mass Spectrom.* **1972**, *6*, 741–747. (b) Ryan, T. M.; Day, R. J.; Cooks, R. G. *Anal. Chem.* **1980**, *52*, 2054–2057. (c) Van Berkel, G. J.; McLuckey, S. A.; Glish, G. J. *J. Am. Soc. Mass Spectrom.* **1992**, *3*, 235–242. (d) Javahery, G.; Petrie, S.; Wincel, H.; Wang, J.; Bohme, D. K. *J. Am. Chem. Soc.* **1993**, *115*, 6295–6301.

(14) (a) McLuckey, S. A.; Van Berkel, G. J.; Glish, G. L. *J. Am. Chem. Soc.* **1990**, *112*, 5668–5670. (b) Ikononou, M. G.; Kebarle, P. *Int. J. Mass Spectrom. Ion Processes* **1992**, *117*, 283–298. (c) Cassady, C. J.; Wronka, J.; Kruppa, G. H.; Laukien, F. H. *Rapid Commun. Mass Spectrom.* **1994**, *8*, 394–400.

(15) (a) Ogorzalek Loo, R. R.; Loo, J. A.; Udseth, H. R.; Fulton, J. L.; Smith, R. D. *Rapid Commun. Mass Spectrom.* **1992**, *6*, 159–165. (b) Ogorzalek Loo, R. R.; Smith, R. D. *J. Am. Soc. Mass Spectrom.* **1994**, *5*, 207–220.

(16) (a) Suckau, D.; Shi, Y.; Beu, S. C.; Senko, M. W.; Quinn, J. P.; Wampler, F. W.; McLafferty, F. W. *Proc. Natl. Acad. Sci. U.S.A.* **1993**, *90*, 790–793. (b) McLafferty, F. W. Private communication. (c) Winger, B. E.; Light-Wahl, K. J.; Rockwood, A. L.; Smith, R. D. *J. Am. Chem. Soc.* **1992**, *114*, 5897–5898.

(17) Covey, T.; Douglas, D. J. *J. Am. Soc. Mass Spectrom.* **1993**, *4*, 616–623.

(18) Gross, D. S.; Williams, E. R. *J. Am. Chem. Soc.* **1995**, *117*, 883–890.

(19) Gross, D. S.; Rodriguez-Cruz, S. E.; Bock, S.; Williams, E. R. *J. Phys. Chem.* **1995**, *99*, 4034–4038.

(20) Chowdhury, S. K.; Katta, V.; Chait, B. T. *Rapid Commun. Mass Spectrom.* **1990**, *4*, 81–87.

(21) Hofstadler, S. A.; and Laude, D. A. *J. Am. Soc. Mass Spectrom.* **1992**, *3*, 615–623.

(22) (a) Lias, S. G.; Liebman, J. F.; Levin, R. D. *J. Phys. Chem. Ref. Data* **1984**, *13*, 695–808. (b) Meot-Ner, M.; Sieck, W. *J. Am. Chem. Soc.* **1991**, *113*, 4448–4460. (c) Decouzon, M.; Gal, J. F.; Maria, P. C.; Raczynska, E. D. *Rapid Commun. Mass Spectrom.* **1993**, *7*, 599–602.

(23) (a) DeFrees, D. J.; McIver, R. T., Jr.; Hehre, W. J. *J. Am. Chem. Soc.* **1980**, *102*, 3334–3338. (b) Gorman, G. S.; Amster, I. J. *J. Am. Chem. Soc.* **1993**, *115*, 5729–5735. (c) Wu, J.; Lebrilla, C. B. *J. Am. Chem. Soc.* **1993**, *115*, 3270–3275. (d) Munson, M. S. B. *J. Am. Chem. Soc.* **1965**, *87*, 2332–2336. (e) Beauchamp, J. L.; Holts, D.; Woodgate, S. D.; Patt, S. L. *J. Am. Chem. Soc.* **1972**, *94*, 2798–2807. (f) Ridge, D. P. *J. Am. Chem. Soc.* **1975**, *97*, 5670–5674. (g) Polley, C. W.; Munson, B. *Int. J. Mass Spectrom. Ion Phys.* **1978**, *26*, 49–60. (h) Smith, D.; Adams, N. G.; Lindinger, W. J. *Chem. Phys.* **1981**, *75*, 3365–3370.

(24) Marshall, A. G.; Wang, T.-C. L.; Ricca, T. L. *J. Am. Chem. Soc.* **1985**, *107*, 7893–7897.

Table 1. Reaction Rates<sup>a</sup> for Proton Transfer from Isolated Cytochrome *c* (*n* + 1)<sup>+</sup> Ions to Reference Bases

reference base <sup>b</sup>	<i>n</i> =														
	3+	4+	5+	6+	7+	8+	9+	10+	11+	12+	13+	14+	15+		
acetone (188.9 kcal/mol)														0.18	
cyclohexanone (194.0 kcal/mol)														<6.7	
2-fluoropyridine (203.9 kcal/mol)										0.063	0.08	0.077	0.14		
3-fluoropyridine (208.6 kcal/mol)								0.0	0.057	0.13	0.25	0.38	0.48		
pyridine (215.7 kcal/mol)					0.10	0.14	0.13	0.29	6.5	<13	<11	<9.1			
<i>tert</i> -butylamine (216.7 kcal/mol)					0.23	0.25	0.47	0.50	<23						
diethylamine (221.4 kcal/mol)					0.24	1.9	<21	<29							
dipropylamine (225.2 kcal/mol)			<i>c</i>	0.0	1.2	<20									
tri- <i>n</i> -butylamine (231.1 kcal/mol)	<i>c</i>	0.17	1.0	0.73	<6.7										
DBN (237.4 kcal/mol)	1.2	10	X <sup>d</sup>	X <sup>d</sup>											
GB <sup>app</sup>	234.3	234.3	228.1	228.1	223.3	219.1	216.2	216.2	212.2	212.2	206.3	206.3	191.5		

<sup>a</sup> All rates are  $\times 10^{-11}$  cm<sup>3</sup>/(mol·s); calculated collision rate is  $7 \times 10^{-8}$  cm<sup>3</sup>/(mol·s). <sup>b</sup> GB values for acetone and cyclohexanone are from ref 22a, 2-fluoropyridine through tri-*n*-butylamine are from ref 22b adjusted to the scale of ref 22a, and DBN (1,5-diazabicyclo[4.3.0]non-5-ene) is from ref 22c. <sup>c</sup> Reaction of all charge states with reference base formed insufficient abundance of (*n* + 1)<sup>+</sup> to measure the GB of *n*<sup>+</sup>. <sup>d</sup> Rates are sufficiently fast that no significant ion abundance for the (*n* + 1)<sup>+</sup> charge state could be isolated.

Table 2. Gas-Phase Basicities (kcal/mol) of Peptides Containing One Basic Amino Acid (Values for Individual Amino Acids Are Given for Comparison)

basic residue <sup>a</sup>	GB(peptide)	GB(individual amino acids) <sup>b</sup>
proline	234.3	221.9
FYGPV		
tryptophan	234.3	221.9
YD-WGFM		
glutamine	237.4	219.5
CYIQNC		
lysine	241.5	226.0
GAGGVGKS		
lysine (c-terminus)	>243.3	226.0
YGGFLK		
arginine		237.4 <sup>c</sup>

<sup>a</sup> The sequence of the peptides is given following the basic residue, using standard one-letter codes for the amino acid residues; the basic residue is indicated in boldface. <sup>b</sup> Values from Amster and co-workers, ref 40, unless specified. <sup>c</sup> Value from Fenselau and co-workers, ref 39, for comparison.

0–120 s at a pressure of  $\sim 3 \times 10^{-7}$  Torr (measured with an uncalibrated ion gauge). The relative error in measured pressure between adjacent bases on our reference base ladder is  $\sim 50\%$ .<sup>25</sup> The absolute pressure in our ion cell could be as much as 2–3 $\times$  lower than that measured at our ion gauge. However, the values for GB<sup>app</sup> we report are obtained from relative rates of reaction with these bases; thus the absolute pressure does not change our assigned GB<sup>app</sup> values. Relative rate constants for proton transfer are obtained by fitting the molecular ion abundance as a function of reaction time to pseudo-first-order kinetics.

For peptides in Table 2, the GB is measured using the kinetic-bracketing method.<sup>26</sup> A proton-bound dimer of each singly protonated peptide molecular ion and each reference base (B) with GB  $\geq 227.9$  kcal/mol (Table 1) is formed by accumulating peptide ions for 15 s in the FTMS cell in which the pressure of base is  $1 \times 10^{-7}$  Torr. The resulting (M + H + B)<sup>+</sup> ion is isolated and excited to a radius of 0.75 cm (10 eV) using SWIFT,<sup>24</sup> and the resulting product ions are detected after a 2.0-s delay. The GB of the peptide is assigned a value halfway between that of the most basic reference base for which the peptide–base complex dissociates to form predominately (M + H)<sup>+</sup> and the least basic reference base for which the complex dissociates to form predominately (B + H)<sup>+</sup>.

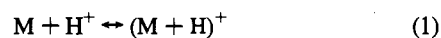
**Calculations.** All computer programs were written in C and run on IBM RS/6000 and Macintosh computers. A standard random number generator based on the subtractive method was employed.<sup>27</sup>

(25) Found, C. B.; Dushman, S. *Phys. Rev.* **1924**, *23*, 734–743.

(26) (a) McLuckey, S. A.; Cameron, D.; Cooks, R. D. *J. Am. Chem. Soc.* **1981**, *103*, 1313–1317. (b) Wu, Z.; Fenselau, C. *J. Am. Soc. Mass Spectrom.* **1992**, *3*, 863–866. (c) Cheng, X.; Wu, Z.; Fenselau, C. *J. Am. Chem. Soc.* **1993**, *115*, 4844–4848. (d) Li, X.-P.; Harrison, A. G. *Org. Mass Spectrom.* **1993**, *28*, 366–371.

## Method

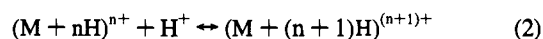
**Definitions.** The proton affinity (PA) and gas-phase basicity (GB) of a neutral molecule, M, and a protonated ion with *n* charges are defined in reactions 1 and 2, respectively. In reaction 1, the attractive



$$-\Delta H_1^\circ = PA(M)$$

$$-\Delta G_1^\circ = GB(M)$$

$$= -(\Delta H_1^\circ - T\Delta S_1^\circ)$$



$$-\Delta H_2^\circ = PA((M + nH)^{n+})$$

$$-\Delta G_2^\circ = GB((M + nH)^{n+})$$

$$= -(\Delta H_2^\circ - T\Delta S_2^\circ)$$

potential for this ion–molecule reaction is relatively short range<sup>28</sup> (Figure 1, top). The barrier to removal of a proton is usually approximately equal to the asymptotic region to the right, representing the separating products. Thus, the PA of a neutral molecule, which is the binding energy of a proton to the neutral molecule, is the energy required to remove a proton from MH<sup>+</sup>. For reaction 2, direct removal of a proton from (M + (n + 1)H)<sup>(n+1)+</sup> has a large reverse activation energy due to the long-range Coulomb repulsion of the separating charged products. A qualitative interaction potential for this reaction is shown in Figure 1, bottom. In contrast to a neutral molecule, the proton affinity of an (M + H)<sup>+</sup> ion, PA(MH<sup>+</sup>), is *not* the energy required to remove a proton from the (M + 2H)<sup>2+</sup> ion.

Methods for measuring the GB and PA of neutral molecules are well established.<sup>23,26,29</sup> These include equilibrium,<sup>29</sup> bracketing,<sup>23</sup> and kinetic methods<sup>26</sup> in which proton transfer reactions with reference bases of known basicity are measured. For the reaction of an (M + H)<sup>+</sup> ion and a neutral base A, where PA(M) = PA(A) (we assume entropic effects are negligible for now so that GB = PA), a qualitative interaction potential is given in Figure 2 (reaction a).

(27) Press, W. H.; Flannery, B. P.; Teukolsky, S. A.; Vetterling, W. T. *Numerical Recipes in Pascal*; Cambridge University Press: Cambridge, 1989.

(28) (a) Aue, D. H.; Bowers, M. T. In *Gas-Phase Ion Chemistry*; Bowers, M. T., Ed.; Academic Press: New York, 1979; Vol. 1, Chapter 3, pp 83–118. (b) McDaniel, E. W. *Collision Phenomena in Ionized Gases*; John Wiley and Sons: New York, 1964. (c) Steinfeld, J. I.; Francisco, J. S.; Hase, W. L. *Chemical Kinetics and Dynamics*; Prentice Hall: New Jersey, 1989.

(29) (a) Taft, R. W. In *Proton Transfer Reactions*; Caldin, E. F., Gold, V., Eds.; John Wiley and Sons: New York, 1975; pp 31–78. (b) Kebarle, P. *Annu. Rev. Phys. Chem.* **1977**, *28*, 445.

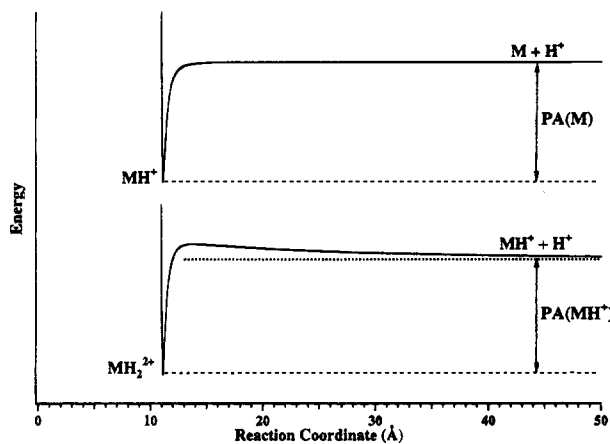


**Figure 1.** Ion-molecule potentials for the reaction of neutral M with a proton (top) and for the reaction of  $MH^+$  with a proton (bottom). The potential is calculated using ADO theory with parameters given in ref 30 and a Coulomb potential with 30 kcal/mol of energy at 11 Å.

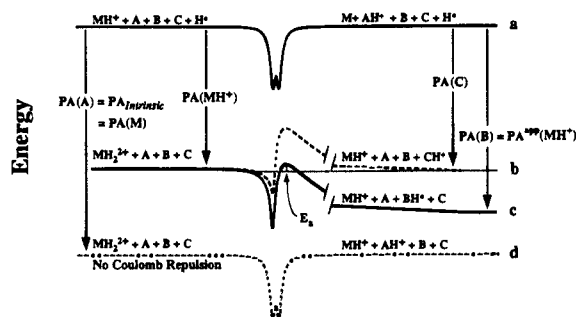


**Figure 2.** Qualitative interaction potentials for proton-transfer reactions of singly and doubly protonated M and neutral reference bases (A, B, and C), where M is a symmetric molecule with two identical sites of protonation. (a) Reaction of  $MH^+$  with A,  $PA(M) = PA(A)$ ; (b) reaction of  $MH_2^{2+}$  with C,  $PA(MH^+) = PA(C)$ ; (c) reaction of  $MH_2^{2+}$  with B,  $PA^{app}(MH^+) = PA(B)$ ; (d) the hypothetical reaction of  $MH_2^{2+}$  with A in the absence of Coulomb repulsion.

Measurement of the GB and PA of multiply protonated ions is made more complicated by the reverse activation barrier. Consider a symmetric molecule M with two identical sites of protonation. Proton transfer from the  $(M + 2H)^{2+}$  ion to a neutral base C (Figure 2, reaction b), where  $PA(C) = PA(MH^+)$ , will be slow under typical experimental conditions due to the high activation barrier for this process. However, the rate of proton transfer can be driven by increasing the basicity of the neutral base such that the activation barrier for proton transfer ( $E_a$ ) is small (Figure 2, reaction c). Thus, proton-transfer reactions of multiply protonated ions with reference bases of known gas-phase basicity under typical experimental conditions do not give the true  $PA(MH^+)$ , but rather an apparent PA ( $PA^{app}(MH^+)$ ) which is greater than  $PA(MH^+)$  by a value approximately equal to the reverse activation barrier for this reaction.<sup>30</sup> The PA of protonated ions could be determined directly if this reverse activation barrier were known; measurement of the kinetic energy release<sup>31</sup> of these separating charged products would indicate this value. Bursley and Pederson<sup>32</sup> have calculated the enthalpy for bringing protonated ammonia and protonated trimethylamine ions from infinite distance to the proton-transfer interaction distance of protonated diaminoethane and found these values to be 77% and 92% of a simple point charge Coulomb model for reaction distances of 7.70 and 8.80 Å, respectively.

**Coulomb Repulsion from Proton-Transfer Reactions.** For multiply protonated ions in which charges are separated by  $\geq 10$  Å, we have proposed that the apparent proton affinity ( $PA^{app}$ ) or apparent

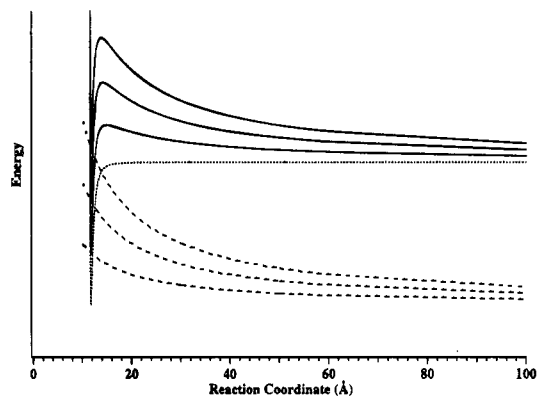


**Figure 3.** Ion-molecule potentials (solid curves) for proton transfer in a multiply protonated ion obtained by adding Coulomb potentials (dashed curves) with 15, 30, and 45 kcal/mol of energy at a distance of 11 Å to an ion-molecule potential (dotted curve) with a 42 kcal/mol well-depth. The barrier heights for proton transfer are 73%, 78%, and 81% of the point-charge Coulomb energy, respectively, and the proton transfer distance decreases by 1.1 Å.

binding energy of a proton to a multiply protonated ion in these ion-molecule reactions is given by eq 3.<sup>18,19</sup> Where  $PA_{Intrinsic,t}$  is the PA of

$$PA_{(n,i)}^{app} \approx PA_{Intrinsic,t} - \sum_{i=1}^n \frac{q^2}{(4\pi\epsilon_0)\epsilon_r r_{i,t}} \quad (3)$$

a molecule protonated at site  $t$  (the PA of the basic site in the absence of other charges), and the second term is the sum of all Coulomb energy experienced by that charge. This should be valid if charges at other sites have negligible effect on the  $PA_{Intrinsic}$  of that site. In the absence of Coulomb interactions, the  $(M + H)^+$  ion would have a PA equal to that of A since both sites of protonation are identical. The interaction potential for this proton-transfer reaction would be the same as that of reaction a, but lower in energy by a value equal to  $PA(A)$  (Figure 2, reaction d). However, with Coulomb repulsion, proton transfer is observable with bases that have proton affinities greater than or equal to that of B (Figure 2, reaction c). It is the difference,  $PA(A) - PA(B)$  ( $=PA(M) - PA^{app}(MH^+)$ ), that should be directly proportional to the Coulomb energy in the  $(M + 2H)^{2+}$  ion.

Because the interaction potential between an ion and a neutral molecule is relatively short range, effects of charges  $\geq 10$  Å from the reaction site have negligible effect ( $< 0.5$  kcal/mol) on the ion-dipole or ion-induced dipole attractive force of these ion-molecule reactions.<sup>18</sup> Thus, the interaction potential for reactions b and c (Figure 2) will be approximately equal to the combined effects of Coulomb and one-charge ion-molecule potentials. If the position of the barrier to proton transfer is not significantly affected by the well-depth of the ion-molecule potential or the magnitude of the Coulomb repulsion, then the difference in  $PA^{app}(MH^+)$  of two  $(M + 2H)^{2+}$  ions with different Coulomb energies but identical  $PA_{Intrinsic}$  will parallel the difference in Coulomb repulsion in these ions. We consider here, briefly, effects of ion-molecule well-depth on barrier height and position in these proton-transfer reactions.

Adding a Coulomb potential with energies of 15, 30, and 45 kcal/mol at a distance of 11 Å to an ion-molecule potential with a 42 kcal/mol well-depth<sup>33</sup> results in potentials with reverse activation barriers of 10.9, 23.5, and 36.6 kcal/mol, respectively (Figure 3). These values are 73%, 78%, and 81% of the true point-charge Coulomb potential, respectively. Reducing the ion-molecule potential to 19 kcal/mol changes the barriers to 10.8, 23.0, and 36.0 kcal/mol; these values are 72%, 77%, and 80% of a Coulomb potential, respectively. These calculations indicate that reducing the ion-molecule well-depth from

(30) Petrie, S.; Javahery, G.; Bohme, D. K. *Int. J. Mass Spectrom Ion Proc.* **1993**, *124*, 145–156.

(31) Cooks, R. G.; Beynon, J. H.; Caprioli, R. M.; Lester, G. R. *Metastable Ions*, Elsevier: Amsterdam, London, New York, 1973.

(32) Bursley, M. M.; Pedersen, L. G. *Org. Mass Spectrom.* **1992**, *27*, 974–975.

(33) The ion-molecule attractive potential is calculated for an ion of  $MW = 130$  Da with data for the typical neutral base dimethylamine (polarizability  $\alpha = 2.32 \times 10^{-40} \text{ J}^{-1} \text{ C}^2 \text{ m}^2$ , dipole moment  $\mu_d = 3.44 \times 10^{-30} \text{ Cm}$ , from: *CRC Handbook of Chemistry and Physics*, D. R. Lide, Ed.; CRC Press: Boca Raton, FL, 1993), using the ADO theory from ref 28a.

42 to 19 kcal/mol reduces the position of the barrier to proton transfer by 0.3 Å and has little effect on the height of this barrier. They also indicate that the change in barrier height roughly parallels, within 11% error, the change in Coulomb repulsion in these ions.

Both the position and height of the barrier depend on the values of polarizability and dipole moments of the base as well as the effective impact parameter ( $b$ ) since these values change the shape of the ion–molecule attractive potential. Reducing  $b$  from 5 Å in the previous calculations to zero changes the calculated barrier heights to 9.1, 20.7, and 33.3 kcal/mol for 15, 30, and 45 kcal/mol Coulomb energy and 42 kcal/mol well-depth. These values are 61%, 69%, and 74% of the Coulomb energy. Similarly, increasing the value of polarizability from  $2.32 \times 10^{-40} \text{ J}^{-1} \text{ C}^2 \text{ m}^2$  (dimethylamine) used in the previous calculations to  $1.43 \times 10^{-39} \text{ J}^{-1} \text{ C}^2 \text{ m}^2$  (triethylamine) lowers the barrier height to 10.3, 22.9, and 35.7 kcal/mol (42 kcal/mol well-depth,  $b = 5 \text{ Å}$ ), which is 69%, 76%, and 79% of the true Coulomb energy. This change in polarizability increases the position of the barrier to proton transfer by 0.4 Å. The dependence of barrier height on these parameters will result in bases, B, with a range of PA's that will undergo proton transfer with  $(M + 2H)^{2+}$  ions near threshold. The semiempirical calculations by Bursey and Pederson<sup>32</sup> on the diprotonated diaminoethane ion indicate that our simple calculations described above underestimate the true height of the barrier. We are investigating these ion–molecule interactions for larger ions more thoroughly using higher level calculations.

Measurements of proton transfer from diprotonated diaminoalkanes ( $^+H_3N(CH_2)_nNH_3^+$ ,  $n = 7-10, 12$ ) to neutral reference bases support our conclusion that Coulomb energy can be obtained from these proton-transfer reactions.<sup>19</sup> The apparent GB of singly protonated diaminoalkanes and GB of the corresponding neutral monoaminoalkane,  $CH_3(CH_2)_nNH_2$ , used as a reference for intrinsic basicity, were measured. The differences in these values were found to decrease from 29.4 to 19.8 kcal/mol for  $n = 7-12$  (charge separation 11–18 Å). In combination with distance between charges calculated from the lowest energy structures obtained by molecular modeling, a dielectric polarizability of  $1.01 \pm 0.07$  was obtained. No systematic change in  $\epsilon_r$  with increasing  $n$  was observed, *i.e.*, the difference,  $GB^{app}(MH^+) - GB(M)$  of the diaminoalkane minus  $GB(M)$  of the monoaminoalkane, equals, within 7% error, the predicted difference in Coulomb repulsion in the  $(M + 2H)^{2+}$  diaminoalkane ions using a point-charge Coulomb model with a constant  $\epsilon_r = 1.01$ . These results provide experimental evidence that the influence of a charge localized  $> 11 \text{ Å}$  away from the reaction center can be fully accounted for by the combined effects of Coulomb repulsion and intrinsic reactivity of that center. They also indicate that effects of polarizability, dipole moment, and impact parameter are relatively small compared to differences in Coulomb energy in these ions. Provided that suitable references for  $PA_{intrinsic}$  can be obtained, the Coulomb repulsion in multiply protonated ions can be obtained from proton-transfer reactions.

These results bring up an intriguing question about the value of the true GB of an  $(M + H)^+$  ion. If both the difference  $PA(A) - PA(B)$  and the value of the reverse activation barrier to thermal proton transfer can be approximated by the Coulomb energy, the difference  $PA(MH^+) - PA(M)$  is approximately twice this value. This brings to question the assumption that the reverse activation barrier in these thermal proton-transfer reactions is a significant portion of the Coulomb energy. For the deprotonation reaction of  $(M + 2H)^{2+}$  ions to form  $(M + H)^+ + H^+$ , calculations indicate that a mechanism in which a  $H^+$  is lost followed by electron transfer to the  $(M + H)^{2+}$  ion at a separation distance of  $\sim 8 \text{ Å}$  is more energetically favorable than direct loss of  $H^+$ , since the former mechanism reduces contributions to the barrier due to Coulomb repulsion.<sup>34</sup> A similar mechanism for our proton-transfer reactions would require formation of an energetically unfavorable hypervalent neutral. Similarly, tunneling of a proton through a wide barrier is highly unfavorable. An estimate of the height of the barrier could be obtained through measurement of the kinetic energy of the separating charged products in these proton-transfer reactions. We are pursuing kinetic energy release measurements for these thermal proton-transfer reactions using the method of Orth, Dunbar, and

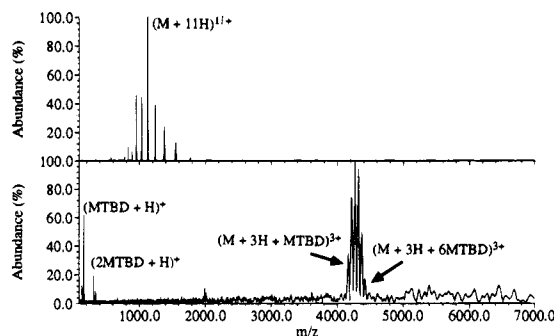


**Figure 4.** ESI-FTMS spectrum of cytochrome *c* from denaturing solution (top) and spectrum of all charge states of cytochrome *c* reacted with MTBD ( $GB = 243.3 \text{ kcal/mol}$ ) for 60 s (bottom).

Riggin.<sup>35</sup> We are also modeling the proton transfer from diprotonated ions to neutral molecules to gain an improved understanding of the dynamics of these reactions.

**Entropic Effects.** To relate GB to Coulomb energy, the difference in  $\Delta S_2$  (reaction 2) and  $\Delta S_{intrinsic}$ , where  $\Delta S_{intrinsic}$  is the entropy of protonation of the neutral protein at a given charge site, must be known. For systems in which independent solvation of the charge sites occurs, then to a first approximation  $\Delta S_2 = \Delta S_{intrinsic}$ . Thus, the Coulomb energy experienced by a proton on site  $t$  is related to GB by eq 4.

$$\text{Coulomb energy} \approx GB_{intrinsic,t} - GB_{(n,t)}^{app} \quad (4)$$

## Results and Discussion

**Measured  $GB^{app}$ .** In a 49.5%/49.5%/1.0% water/methanol/acetic acid solution, cytochrome *c* is denatured;<sup>36</sup> the ESI-FTMS spectrum obtained from this solution has a charge distribution from 7+ to 16+ (Figure 4, top). Each of these ions is readily isolated using SWIFT and the relative rates of proton transfer between each of these isolated charge states and the reference bases is measured. These values are given in Table 1. Charge states below 7+ are formed in negligible abundance directly by electrospray ionization. To produce lower charge states, all ions are reacted with a reference base in the ion cell. Using this method, charge states as low as 3+ are formed. This ion undergoes no further proton-transfer reaction with the most basic reference molecule for which a GB has been reported, MTBD<sup>37</sup> ( $GB = 243.3 \text{ kcal/mol}$ ).<sup>22c</sup> Adducts of up to 6 MTBD molecules are formed with the 3+ ion with 60 s reaction time (Figure 4, bottom). This high extent of clustering is somewhat surprising given the steric bulk of MTBD. The 4+ ion also forms adducts with up to 3 DBN molecules ( $GB = 237.4 \text{ kcal/mol}$ );<sup>22c</sup> these adducts undergo proton transfer to form 3+ ions with 30 s reaction delays. No adducts are observed for the higher charge states. Rates of proton transfer for charge state 3+ to 15+ are given in Table 1.

Proton-transfer rates of these multiply protonated ions show increases in reactivity with increasing GB of the reference bases. However, less distinct “jumps” in reactivity between bases of increasing GB are observed than was the case for doubly protonated gramicidin *s*.<sup>18</sup> This lack of a distinct change in reactivity has been observed previously for proton-transfer reactions of singly charged poly(glycine) with increasing chain length<sup>23c</sup> and complicates the assignment of GB. As an

(35) (a) Orth, R.; Dunbar, R. C.; Riggin, M. *Chem. Phys.* **1977**, *19*, 279–288. (b) Knott, T. F.; Riggin, M. *Can. J. Phys.* **1977**, *52*, 426–435. (c) Mauclair, G.; Derai, R.; Feinstein, S.; Marx, R. *J. Chem. Phys.* **1984**, *80*, 4901–4906. (d) O’Keefe, A.; Parent, D.; Mauclair, G.; Bowers, M. T. *J. Chem. Phys.* **1984**, *80*, 4901–4906.

(36) (a) Theorell, H.; Akesson, A. *J. Am. Chem. Soc.* **1941**, *63*, 1804–1820. (b) Babul, J.; Stellwagen, E. *Biochemistry* **1972**, *11*, 1195–1200.

(37) MTBD = 1,3,4,6,7,8-hexahydro-1-methyl-2H-pyrimido[1,2-a]-pyrimidine.

(34) Gill, P. M. W.; Radom, L. *J. Am. Chem. Soc.* **1988**, *110*, 5311–5314.

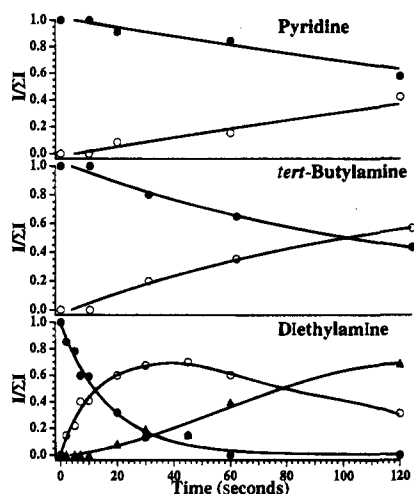


**Figure 5.** Kinetic curves for the reaction of cytochrome *c* 9+ with pyridine (GB = 215.7 kcal/mol, top), *tert*-butylamine (GB = 216.7 kcal/mol, middle), and diethylamine (GB = 221.4 kcal/mol, bottom): (●) 9+, (○) 8+, (▲) 7+.

example, normalized ion abundances for the proton-transfer reactions of the 9+ ion with three bases are shown in Figure 5. No measurable proton transfer is observed for compounds with GB less than that of 3-fluoropyridine (GB = 208.6 kcal/mol). Proton transfer to pyridine (GB = 215.7 kcal/mol) and *tert*-butylamine (GB = 216.7 kcal/mol) both fit pseudo-first-order kinetics with rate constants of  $1.4 \times 10^{-12}$  and  $2.5 \times 10^{-12}$   $\text{cm}^3/(\text{mol}\cdot\text{s})$ , respectively. Proton transfer to diethylamine (GB = 221.4 kcal/mol) is significantly faster ( $1.9 \times 10^{-11}$   $\text{cm}^3/(\text{mol}\cdot\text{s})$ ), occurring at a rate 7.6 times that with *tert*-butylamine. We define reactions with a rate constant less than  $3.6 \times 10^{-12}$   $\text{cm}^3/(\text{mol}\cdot\text{s})$  as "slow" and those with a higher rate constant as "fast". Thus, the  $\text{GB}^{\text{app}}$  of the 8+ ion (measured by proton transfer from 9+ ion) is assigned a value of 219.5 kcal/mol, half-way between the GB of *tert*-butylamine and diethylamine. Although these  $\text{GB}^{\text{app}}$  assignments are somewhat arbitrary, the error introduced by this method is systematic. This offset is incorporated into our intrinsic basicity values and has negligible effect on the ability to extract Coulomb repulsion or dielectric polarizabilities.

The kinetic data for all charge states fit, within experimental error, a single rate constant, consistent with a single gas-phase structure for each charge state. No correction for differences in the collisional encounter rate for the different charge states of these ions is made. The Langevin model predicts that the number of collision encounters should increase nearly linearly with charges. Thus, higher charge states are expected to have higher collisional cross sections. However, not all the charge sites in these multiply protonated ions are identical, e.g., protons located on very basic sites that experience relatively little Coulomb energy would be expected to be unreactive. Our calculations indicate that the number of reactive protons in cytochrome *c* changes by less than a factor of 2.5 from the 4+ to 16+ ions.<sup>38</sup>

The assigned values of  $\text{GB}^{\text{app}}$  for each charge state are given in Table 1. For charge states below 6+, the  $\text{GB}^{\text{app}}$ s are increasingly greater than those of the individual basic amino acids at which protonation is primarily expected to occur. Although the GB of Arg, the most basic of the amino acids, is 237.4 kcal/mol,<sup>39</sup> there are only two Arg residues in cytochrome *c*. Thus, for charge states above 3+ (we assign one charge to

the heme), protonation is expected to occur at the other basic residues. The basicity of the 3+ ion is 234.3 kcal/mol, 8 kcal/mol higher than the next most basic amino acid Lys (GB = 226.0 kcal/mol).<sup>40</sup> The higher basicity of the protein ion indicates that the charges are stabilized through intramolecular interactions<sup>18,41</sup> even in the presence of other charges on the ion and is consistent with independent solvation of the charge sites. Thus, the intrinsic basicity of the charge sites in this protein is substantially higher than what would be predicted just taking into account the GB of the individual amino acids.

To determine the effects of solution composition on our ion  $\text{GB}^{\text{app}}$  measurements, cytochrome *c* was electrosprayed from pure water in which cytochrome *c* is in its native conformation.<sup>36</sup> A charge distribution of 11+ to 7+ is typically observed. The  $\text{GB}^{\text{app}}$  of the 10+ to 7+ ions were measured and found to be the same within experimental error as those measured for cytochrome *c* electrosprayed from a denaturing water/methanol/acetic acid solution. Similar results have been reported by Smith and co-workers,<sup>15b</sup> who observed no significant difference in reactivity in the interface region of whole populations of charge states of ubiquitin, cytochrome *c*, and myoglobin for ions formed from native and denaturing solutions.

**Ion Detection Efficiency.** Proton transfer from cytochrome *c* ions with *n* protons to neutral base molecules generates protonated base and the (*n* - 1) charge state of cytochrome *c* in exactly equal abundance. The relative intensity of these ions observed in the spectrum, normalized for the number of charges on the ion, is a direct measurement of the relative detection efficiency of these different mass species. We find that the relative intensity of protonated base to deprotonated cytochrome *c* ion decreases with increasing detection transient length, presumably due to scattering loss of the light ion or to resonant proton transfer to neutral base in the system. Averaging results for the reaction of 9+ through 12+ ions (*m/z* 1031–1374) with three bases indicates that the relative detection efficiency of (B + H)<sup>+</sup> ions (*m/z* 74–80) to the higher mass ions is 0.06, 1.7, and 3.1 at 50 ms, 6.3 ms, and 0.4–3.1 ms average transient detection lengths, respectively. In order to minimize the effect of differences in detection efficiency, reaction rates are obtained from decreases in cytochrome *c* *n*+ abundance and the increase of the (*n* - 1) charged species (normalized for charge), rather than the appearance of protonated base molecules. The ratio of detection efficiencies of 3.1 for the short transient times is larger than the value of 2.3 obtained for reactions of gramicidin *s* under nearly identical experimental conditions.<sup>18</sup> This difference indicates that ion signal may not increase linearly with charge on an ion present in an ensemble. We are investigating this phenomenon further.

**Estimates of  $\text{GB}_{\text{intrinsic}}$ .** In order to estimate the intrinsic basicity of charge sites in a protein, the GBs of several small peptides (5–9 residues), each containing one basic residue, were measured. These small peptides form base attached adducts with the more basic reference molecules. For these ions, the GB is measured with the kinetic method.<sup>26</sup> Typical results for dissociation of the (M + H + B)<sup>+</sup> ion of the Lys containing peptide Hu-ras<sup>Hla</sup> (GAGGVGKS) and three reference bases are shown in Figure 6. For 10-eV dissociations of the proton-bound dimer of peptide and DBU (1,8-diazabicyclo[5.4.0]undec-7-ene, GB = 239.7 kcal/mol),<sup>22c</sup> the abundance of the (B + H)<sup>+</sup> ion is less than that of the (M + H)<sup>+</sup> ion. This ratio is inverted for

(40) Gorman, G. S.; Spier, J. P.; Turner, C. A.; Amster, I. J. *J. Am. Chem. Soc.* **1992**, *114*, 3986–3988.

(41) (a) Aue, D. H.; Webb, H. M.; Bowers, M. T. *J. Am. Chem. Soc.* **1973**, *95*, 2699–2701. (b) Kebarle, P. *Annu. Rev. Phys. Chem.* **1977**, *28*, 445–476. (c) Meot-Ner, M.; Hamlet, P.; Hunter, E. P.; Field, F. H. *J. Am. Chem. Soc.* **1980**, *102*, 6393–6399.

(38) Manuscript in preparation.

(39) Wu, Z.; Fenselau, C. *Rapid Commun. Mass Spectrom.* **1992**, *6*, 403–405.

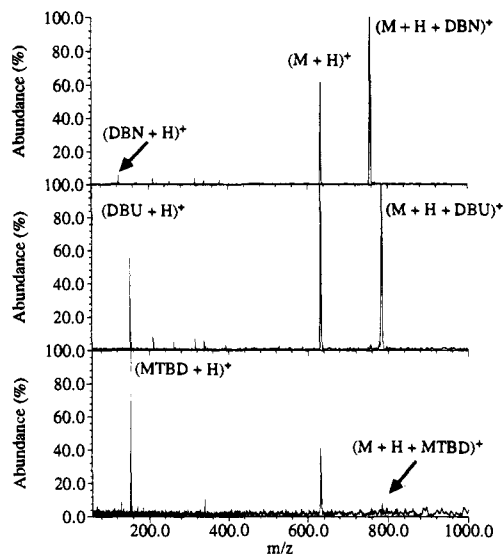


**Figure 6.** Products of dissociation of proton-bound dimers of Hura ras<sup>Ha</sup> with DBN (GB = 237.4 kcal/mol, top), DBU (GB = 239.7 kcal/mol, middle), and MTBD (GB = 243.3 kcal/mol, bottom).

dissociation of the proton-bound dimer of this peptide and MTBD. This indicates that the basicity of this peptide is between that of these two reference bases, or 241.5 kcal/mol. For the Lys containing peptide Leucine Enkephalin-Lys (YG-GFLK), dissociation of the protonated dimer with MTBD results in a (M + H)<sup>+</sup>/(B + H)<sup>+</sup> ratio of 2.9, indicating that the GB of the peptide is slightly more than that of MTBD, i.e. GB > 243.3 kcal/mol. Similarly, the GB's of the other basic amino acid containing peptides were measured and are reported in Table 2.

For Pro and Trp containing peptides, an increase in GB of 12.4 kcal/mol over that of the corresponding individual amino acids is observed. For Gln and Lys, we find an increase of ~17 kcal/mol. We attribute this larger increase in GB of Gln and Lys to the higher flexibility of the charged side-chain nitrogen that should make possible more favorable stabilizing interactions. In contrast, the charged nitrogen in Pro and Trp is fixed in a relatively rigid ring that is more difficult to orient for maximum stabilization. Higher basicity due to charge solvation is also observed for the cyclic peptide gramicidin s,<sup>18</sup> indicating that the terminal groups are not required for this increased stabilization. Lebrilla and co-workers<sup>23c</sup> reported an increase in GB of 6 kcal/mol for poly(glycine)<sub>n</sub> (n = 2–5) over that of glycine. This is in contrast to results reported by Fenselau and co-workers,<sup>26b</sup> who found that the PA increased by 32 kcal/mol from n = 1 to 10, although at a diminishing rate. Both of these studies indicate that the intramolecular solvation and stabilization of a single proton in a polypeptide will have a maximum value which will not increase with further increase in polypeptide chain length. Clearly, investigation of additional and larger peptides should provide more accurate values of this stabilization energy.

Our results indicate that the intrinsic basicity of Lys in a protein is at least 17 kcal/mol higher than that of an individual Lys molecule. This differs substantially from the conclusions of Cassidy *et al.*, who report the intrinsic basicity of Lys in the protein ubiquitin is ±10 kcal/mol of an individual Lys molecule.<sup>14c</sup>

Peptides containing Arg were not studied since Arg is only 5.9 kcal/mol less basic than MTBD, the most basic reference molecule for which a value of GB has been reported.<sup>22c</sup> The increased basicity due to intramolecular solvation is not measurable for large peptides containing this highly basic residue.

**Calculated GB<sup>app</sup>.** To understand the influence of charge

state and ion structure on GB<sup>app</sup>, we present a relatively simple model that explains these effects quantitatively. Since Coulomb energy changes with distance between charges, this value depends on the conformation of the ion. We model two extremes: first, a linear string model in which Coulomb energy is minimized, and second, the folded native structure in which Coulomb energy for a given charge state is significantly greater.

For each charge state, multiple configurations of charge on the ion are expected to be produced in the electrospray ionization process. McLafferty and co-workers<sup>16</sup> have reported that cytochrome c ions formed by electrospray ionization from a denaturing solution undergo first-order exchange of deuterium for hydrogen (up to 133 of 198 exchangeable hydrogens) upon reaction with D<sub>2</sub>O in the gas phase. Since exchange is expected to occur significantly faster at charge sites, these results indicate that scrambling of hydrogens between all possible sites of protonation in the ion occurs in the gas phase. It is expected that protons have at least some interaction with other charge sites as well. Thus, under near-thermal conditions, the lowest free-energy charge configurations should be favored.

To calculate these configurations for each charge state, we assign charges to any of the amino acid residues in the ion such that the GB<sup>app</sup> of each charge state is maximized. This is accomplished by minimizing expression 5. In a simplistic

$$\sum_{\substack{ij \\ i>j}}^n \frac{q^2}{(4\pi\epsilon_0)\epsilon_r r_{ij}} - \sum_{i=1}^n GB_{\text{Intrinsic},i} \quad (5)$$

approximation, we assign GB<sub>Intrinsic</sub> for Pro, Trp, Gln, and Lys to be the values of these residues in the small peptides (234.3, 234.3, 237.4, and 241.0 kcal/mol, respectively, *vide supra*). For Arg and His, we add the average increase in basicity measured in the small peptides, 15 kcal/mol, to that of the corresponding individual amino acid<sup>42</sup> resulting in a GB<sub>Intrinsic</sub> for these amino acids of GB = 252.4 and 242.7 kcal/mol, respectively. For all other residues, we use a GB<sub>Intrinsic</sub> = 221.6 kcal/mol which corresponds to the estimated value for protonation of a backbone amide<sup>43</sup> plus 15 kcal/mol to account for solvation energy. Implicit in this approximation is that the charge solvation that takes place in a small peptide is the same as that which occurs in a protein, independent of whether the protein is folded or denatured. It is energetically favorable for charge solvation to occur even in highly charged ions.<sup>38</sup> In a denatured conformation, solvation of protonated side chains could occur through interactions with two backbone carbonyl oxygens or with adjacent polarizable side-chain residues. A folded ion conformation would presumably enhance these stabilizing interactions, although this stabilization will not increase beyond some maximum value. To test whether the GB<sub>Intrinsic</sub> values are reasonable for a denatured protein, the GB<sup>app</sup> of small doubly protonated peptide ions with only two identical interior basic sites (separated by >10 Å) could be measured; the structure of these ions would presumably be largely linear due to the Coulomb repulsion between the charges.

The "denatured" conformation is modeled as an elongated linear string in which the amino acid residues are separated by 3.8 Å.<sup>2</sup> For the heme group, a single charge is placed between residues 14 and 15, offset by 5 Å from the backbone for all charge states. Thus, we assign the charge state of an ion as (M + nH)<sup>(n+1)+</sup>. This model differs from that of Rockwood *et al.*<sup>3b</sup> in that charges are not evenly distributed along the "string"; charge location depends on the intrinsic reactivity of various

(42) Values for the individual amino acids Arg and His were obtained from ref 39 and 40, respectively.

(43) Wu, Z.; Fenselau, C. *Tetrahedron* 1993, 49, 9197–9206.

sites and hence the sequence of the protein. The "native" conformation is modeled using the X-ray crystal structure;<sup>44</sup> coordinates of the basic side-chain nitrogens and the backbone carbonyl oxygens are used for the basic side-chain amino acids and for all other amino acids, respectively. A single charge is placed at the coordinates of the iron in the heme group for all charge states.

For a protein with  $r$  residues and  $n$  charges, the number of possible charge configurations is given by eq 6. For equine

$$\text{no. of charge configurations} = \frac{\prod_{i=0}^{(n-1)} (r-i)}{n!} \quad (6)$$

cytochrome  $c$  which has 104 residues, there are  $\sim 10^{21}$  possible ways to assign charges for the 20+ ion. Thus, a direct calculation of energies of all the possible configurations becomes impractical for all but small peptides/proteins or low charge states. To overcome this difficulty, we developed a pseudo-random-walk algorithm to find the lowest energy configuration more efficiently.

An initial configuration of  $n$  charges is arbitrarily selected and the ion free energy is calculated. One charge is then randomly selected and given an equal probability of being moved within 10 residues of its current location in the direction of either the N or C terminus; the charge is moved to either the nearest unoccupied basic residue or to a random unoccupied residue (including non-basic sites) with an 85% and 15% probability, respectively. If the free energy of this new configuration is less than the original free energy, the move is accepted and this process repeated. In order to avoid local minima which do not represent lowest energy structures, higher energy configurations are accepted with a probability given by eq 7, where  $\Delta E_T$  is the increase in free energy for this new

$$\text{probability} = -\frac{1}{N}\Delta E_T + 1 \quad (7)$$

structure, and  $N$  is 16 and 50, 90% and 10% of the time, respectively (a negative probability is assigned a value of 0). This process is repeated  $10^6$ – $10^7$  times and all of the lowest energy configurations within 3 kcal/mol are tabulated. The  $GB^{\text{app}}$  of each proton in each lowest energy configuration is computed by subtracting the total Coulomb repulsion on the proton from its value of  $GB_{\text{Intrinsic},i}$ . The overall  $GB^{\text{app}}$  for the charge configuration is assigned as that of the most easily removed proton (lowest  $GB^{\text{app}}$ ). We assign the  $GB^{\text{app}}$  for the charge state as the average of the  $GB^{\text{app}}$ s of all the charge configurations within 3 kcal/mol of the lowest free energy.

To test whether this algorithm is finding the lowest energy configurations, the energies of all possible configurations for the 3+ to 13+ charge states with  $\epsilon_r = 1.0$  were determined.<sup>45</sup> For the 14+ through 22+ charge states, energies for all possible combinations of charge were found by limiting the charge assignments to only basic residues. The pseudo-random-walk algorithm found either the same lowest energy configurations or lower energy configurations corresponding to placing charges on "backbone" sites of non-basic residues for the higher charge states.

To confirm that the lowest energy structures are found with the pseudo-random-walk algorithm independent of the initial

charge assignment, several initial configurations were tried. For  $n = 15$ – $21$  charge states, four configurations corresponding to charges on the first  $n$  positions of the N-terminal end, the last  $n$  positions on the C-terminal end, the  $n$  consecutive positions in the middle, and the  $n$  charges spread evenly, but avoiding initial placement on any basic sites were tried. For each of these initial charge assignments, the same low-energy configurations were found. Convergence to the lowest energy configuration requires on average  $10^5$  iterations for charge states greater than 15+. A total of  $5 \times 10^6$  iterations are typically used for each charge state. With  $10^8$  iterations for the 18+ to 21+ charge state, no additional low-energy structures were found. From these tests, we infer that the lowest energy configurations for each charge state are obtained.

The calculated  $GB_{\text{Intrinsic}}$  and  $GB^{\text{app}}$  we report are averages of those for all configurations within 3 kcal/mol of the lowest energy structure. Because of the similar energies, multiple charge configurations for each charge state are expected even under thermal conditions. Averaging the lowest energy configurations is expected to provide a more accurate value. The number of charge configurations within this energy range depends on the number of charges on the ion. For example, we find that the 2+ and 3+ ion have 2 and 1 configurations, respectively. In contrast, an average of 76 charge configurations are found for 5+ to 9+ ions, and an average of 20 are found for all other charge states.

**Dielectric Polarizability.** With our elongated string model of cytochrome  $c$  and an  $\epsilon_r = 1.0$ , we find that our calculated values of  $GB^{\text{app}}$  become increasingly lower than our measured values for higher charge states (Figure 7). For example, the 13+ charge state has a calculated  $GB^{\text{app}}$  of 173 kcal/mol, 42 kcal/mol lower than the measured value. All higher charge states have calculated  $GB^{\text{app}}$  less than that of methanol<sup>22a</sup> (174.1 kcal/mol) and would be expected to undergo proton transfer with this molecule. This reaction is not observed experimentally. The elongated structure used in our calculations *minimizes* the Coulomb energy so that our calculated  $GB^{\text{app}}$  should *overestimate* the actual  $GB^{\text{app}}$ . Thus, we conclude that the dielectric polarizability of cytochrome  $c$  ions in vacuum must be greater than 1.0.

In order to obtain a value of  $\epsilon_r$ , the calculated values are fit to the experimentally measured basicities. This is done by calculating a value of  $\epsilon_r$  for each charge state from eq 8. These

$$\left( \frac{GB_{\text{Intrinsic}} - GB^{\text{app}}_{\text{Calculated}}}{GB_{\text{Intrinsic}} - GB^{\text{app}}_{\text{Experimental}}} \right) \epsilon_{r,n-1} = \epsilon_{r,n} \quad (8)$$

values are averaged and new charge configurations determined using this new value, since the lowest energy configuration and hence the calculated  $GB^{\text{app}}$  is a function of  $\epsilon_r$ . This process is iterated until  $\epsilon_r$  converges ( $n$  iterations). For cytochrome  $c$ , we find  $\epsilon_r = 2.0 \pm 0.2$ . Figure 7 shows the fit of calculated  $GB^{\text{app}}$  to the experimentally determined values with  $\epsilon_r = 2.0$ . This value is a lower limit since our linear model minimized Coulomb repulsion, although slight changes in conformation, such as bending the ion, have negligible effect on this value (*vide infra*). It is important to note that this value of  $\epsilon_r$  is an effective constant used to fit our experimental  $GB^{\text{app}}$  data for this gas-phase protein to our point charge Coulomb model. To the extent that the approximations and assumptions in our method are valid, this value of  $\epsilon_r$  is the lower limit to the dielectric polarizability of cytochrome  $c$  ions in vacuum. This value is higher than that for gramicidin  $s$  ( $\epsilon_r < 1.2$ ),<sup>18</sup> but at the lower limit of the range of 2–4 predicted by theory for the interior of a protein.<sup>11</sup> This lower value can be attributed to the effects of the surrounding medium, which, for our gas-phase ions, is vacuum (vacuum

(44) (a) Bushnell, G. W.; Louie, G. V.; Brayer, G. D. *J. Mol. Biol.* **1990**, *214*, 585–595. (b) Brayer, G. D. Personal communication.

(45) Testing was performed on tuna cytochrome  $c$  using  $GB_{\text{Intrinsic}}$  values corresponding to those of the individual amino acids (ref 40).



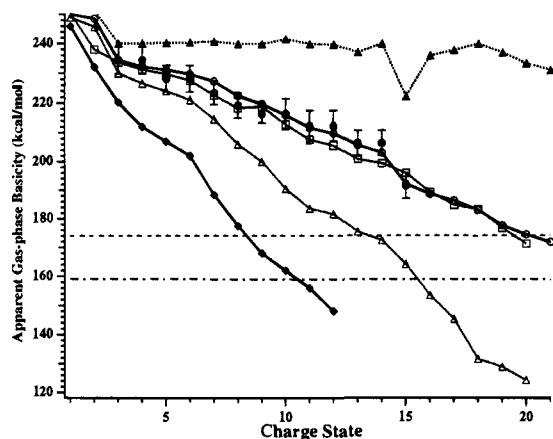


**Figure 7.** Apparent gas-phase basicity as a function of charge state of cytochrome *c* ions, measured (●); calculated, linear ( $\epsilon_r = 1.0$ ,  $\Delta$ ); best fit  $\epsilon_r = 2.0$ ,  $\circ$ ); intrinsic,  $\blacktriangle$ ; calculated, X-ray crystal structure ( $\epsilon_r = 2.0$ ,  $\blacklozenge$ ); calculated,  $\alpha$ -helix ( $\epsilon_r = 4.1$ ,  $\square$ ). The dashed line indicates GB of methanol (174.1 kcal/mol) and the dash-dot line indicates GB of water (159.0 kcal/mol).

permittivity = 1.00). Our results indicate a denatured conformation in the gas phase (*vide infra*), which would maximize these effects. In addition, self-solvation of the charge in the gas phase reduces the ability of these polar groups to orient themselves to reduce the electric field induced by the charge. Both of these latter factors are expected to result in a reduction in  $\epsilon_r$  over a protein in its native conformation. In order to obtain a value of  $\epsilon$  for the interior of a protein which can be used in the dielectric continuum model, effects of both the surrounding medium (vacuum) and ion conformation must be determined. We are investigating this, as well as the effects of ion conformation, further using classical electrostatic models.

**Charge Configuration.** Equine cytochrome *c* has 32 residues which contain basic side chains (2 Arg, 19 Lys, 3 His, 4 Pro, 1 Trp, and 3 Gln). In all lowest free energy charge configurations obtained for the linear structure with  $\epsilon_r = 2.0$ , protonation for charge states below 16+ occurs exclusively on the basic residues Arg, His, Lys, and Pro (Figure 8). Protonation occurs on the C-terminal residue in charge states 16+ to 21+ in almost all of the lowest energy configurations. In contrast, protonation on the N-terminus is indicated only in the 20+ charge state, presumably due to the greater density of basic residues near the N-terminus. Protonation of non-basic residues is also found to occur at residues 95, 96, and 103, which are charged in less than 10% of all of the lowest energy charge configurations found in 16+ to 21+ ions. In the crystal structure, protonation occurs exclusively on basic sites for all charge states up to 12+.

In the linear model, deprotonation occurs primarily at sites located near the center of the molecule, where Coulomb repulsion is greatest. For the 16+ charge state, the least basic proton is a backbone site in every configuration, hence the  $GB_{\text{intrinsic}}$  of the 15+ ion is 220.5 kcal/mol, significantly lower than that of the other  $GB_{\text{intrinsic}}$  values (Figure 7). For higher charge states, the Coulomb repulsion at a charged basic residue is sufficiently high to cause deprotonation at these sites 90% of the time.

**Protein Conformation.** A "rigid rod" type of structure for multiply charged ions is not entirely physically reasonable. To determine the effects of bending the ion on  $GB^{\text{app}}$ , cytochrome *c* is modeled as an arc with curvature ranging from 10 to 180°. For the 20+ charge state, a 180° arc decreases the basicity by 5 kcal/mol. This relative insensitivity of  $GB^{\text{app}}$  on bending the ion structure is primarily due to the central position of the least

basic proton. Bending the ion has minimal effect on the Coulomb energy experienced by these protons. These calculations were performed with a dielectric polarizability of 1.0; a higher value would decrease the effect of bending even further. Thus, our extended ion model is not significantly affected by allowing the ion to bend.

Modeling cytochrome *c* ions using the X-ray crystal coordinates<sup>44</sup> and an  $\epsilon_r = 2.0$  results in significantly lower  $GB^{\text{app}}$ s due to the closer proximity of charges (Figure 7). For 8+, a difference in basicity of 43 kcal/mol from the linear structure is predicted using the same value of  $\epsilon_r = 2.0$  for both these structures. Under our experimental conditions, we find no difference in  $GB^{\text{app}}$  when electro-spraying from water (native) or water/methanol/acetic acid (denatured). Fitting our experimental  $GB^{\text{app}}$ s to the crystal structure results in an  $\epsilon_r = 12 \pm 2$ . We find this to be an unreasonably high value based on previously reported theoretical values of 2–4 for the interior of a protein.<sup>11</sup> These results indicate that these ions are significantly denatured in the gas phase.

Clearly, the value of  $\epsilon_r$  we obtain from our calculations depends on the ion conformation modeled. With cytochrome *c* modeled as an  $\alpha$ -helix,<sup>46</sup> the best fit to our experimental data is obtained using an  $\epsilon_r = 4.1 \pm 0.3$  (Figure 7). We are not able to distinguish between a fully denatured ion ( $\epsilon_r = 2.0$ ) and one that is entirely in an  $\alpha$ -helical conformation ( $\epsilon_r = 4.1$ ). Partial helical structure could be fit using an intermediate value of  $\epsilon_r$ . However, the data for all charge states can be fit using one ion conformation and a single value of  $\epsilon_r$  indicating a common ion structure for all charge states. It is also possible that some tertiary structure is formed in the lower charge states and that the  $\epsilon_r$  for these more compact structures is higher. We are investigating the effects of gas-phase ion conformation on  $\epsilon_r$  and these results will be reported elsewhere.

Gas-phase  $D_2O$  exchange experiments of McLafferty and co-workers<sup>16</sup> indicate that as many as four different conformers of cytochrome *c* exist in the gas phase. More recent results<sup>16b</sup> indicate that cytochrome *c* ions formed from denaturing solution may retain partially folded conformations in the gas phase, although the exact nature of these structures is not known. Covey and Douglas<sup>17</sup> reported collisional cross-sections of the 9+ ion of cytochrome *c* electro-sprayed from a highly aqueous (native) and more highly organic (denatured) solution to be 1800 and 2370 Å<sup>2</sup>, respectively. Our unsuccessful attempts to measure a more compact conformer when electro-spraying from aqueous solution indicates that ions are becoming denatured prior to the  $GB^{\text{app}}$  measurements under our experimental conditions. Lowering the temperature of the heated metal capillary to 160 °C, the lowest temperature at which ion signal is still observed, had no effect on our measurements. We are investigating all aspects of our ion introduction system to form "cooler" ions and the use of gas-phase H/D exchange to distinguish conformers prior to  $GB^{\text{app}}$  measurements.

**Maximum Charge State.** It is interesting to note that our modeling with  $\epsilon_r = 2.0$  accounts for the highest charge states observed in the literature for both an aqueous (native) and water/methanol/acetic acid solution (denatured),<sup>47</sup> 11+ and 21+, respectively. The calculated  $GB^{\text{app}}$  of the 21+ ion ( $GB^{\text{app}} = 173$  kcal/mol) in the denatured form is slightly below that of methanol ( $GB = 174.1$  kcal/mol).<sup>22a</sup> Thus, proton transfer from the 22+ ion to neutral methanol should be highly exothermic

(46) A standard right-handed  $\alpha$ -helix was modeled with 3.6 residues per turn and a translation along the z-axis of 1.5 Å per residue. In a simplifying assumption, all charges were placed at the position of the backbone carbonyl oxygens.

(47) Smith, R. D.; Loo, J. A.; Ogorzalek Loo, R.; Busman, M.; Udseth, H. R. *Mass Spectrom. Rev.* **1991**, *10*, 359–451.



which can be polarized or orient themselves to reduce the electric field. This could also be interpreted as delocalization of charge. Our method relies on a number of assumptions and estimated values such as  $GB_{\text{intrinsic}}$  for each of the sites or protonation. Improved measurements of these values as well as a better understanding of the dynamics of these proton-transfer reactions will undoubtedly result in more accurate values of both the Coulomb repulsion and  $\epsilon_r$ . Nevertheless, our model appears to accurately account for the proton-transfer reactivity of multiply protonated cytochrome *c* ions, as well as the maximum charge state observed for this and other proteins formed by electrospray ionization.

Coulomb energy increases exponentially with the number of protons on an ion. Our calculations indicate that the Coulomb energy in a denatured 21+ ion is 24 eV. For an 11+ ion in its native structure, the Coulomb energy is 20 eV. This large electrostatic contribution to ion zero-point energy accounts for the increased reactivity and dissociation of these highly protonated ions.

Protonation is found to occur primarily on the most basic side-chain amino acids, although protonation on the backbone for charge states above 16+ is indicated. The high basicity of the lower charge states is consistent with intramolecular or self-solvation of the protonation sites resulting in an increase in basicity of 13–18 kcal/mol over that of the corresponding individual amino acid. In solution, these primarily basic sites are solvated by water,<sup>2</sup> indicating a fundamental difference between the solution and gas-phase conformation of protein ions.

Our calculations indicate that the apparent GB is highly dependent on protein conformation; a more compact structure

of a given charge state will have a lower  $GB^{\text{app}}$  than a denatured conformer due to increased Coulomb repulsion. For the 8+ charge state of cytochrome *c*, our calculations indicate that the difference in  $GB^{\text{app}}$  between the native and denatured ion is 43 kcal/mol, using  $\epsilon_r = 2.0$  for both these ion structures. We find no measurable difference in  $GB^{\text{app}}$  of cytochrome *c* ions electrosprayed from aqueous and highly organic solutions in which the protein conformation is native and denatured, respectively, indicating a denatured gas-phase conformation for ions produced from either solution. We are investigating experimental conditions that might favor the native conformation, and are pursuing these  $GB^{\text{app}}$  measurements and calculations with other proteins for which different gas-phase conformations have been reported.<sup>15b,16</sup>

**Acknowledgment.** The authors thank J. I. Brauman, D. J. Leahy, D. M. Neumark, P. B. O'Connor, W. D. Price, and R. J. Saykally for helpful discussions and G. D. Brayer for generously providing the X-ray crystal structure coordinates for equine cytochrome *c* and gratefully acknowledge generous financial support from the Arnold and Mabel Beckman Foundation (M1652), the National Science Foundation (CHE-9258178), the Analytical Chemists of Pittsburgh (M1601), the Exxon Foundation (13605), Extrel FTMS Waters Millipore Corp., Finnigan MAT through sponsorship of the 1994 American Society for Mass Spectrometry Research Award (E.R.W.), W. R. Grace, Co. (D. S. G.), and the DOED (P. D. S.) for fellowship support.

JA943164M